A New Frequency Hopping Signal Detection of Civil UAV Based on Improved K-Means Clustering Algorithm

JIAQUAN YE[1], JIE ZOU[1], JING GAO[1], GUOMIN ZHANG[2], MINGMING KONG[ID][2], ZHENG PEI[ID][2], AND KAITAO CUI[1]
[1] The Second Research Institute of CAAC, Chengdu 400000, China
[2] College of Computer Science and Software Engineering, Xihua University, Chengdu 610039, China

Corresponding author: Mingming Kong (kongming000@126.com)

ABSTRACT The rapid development of civil UAV promotes the social and economic development, and the frequent "flying illegally" events has brought great challenges to aviation safety and government supervision. The frequency hopping communication system used in UAV data transmission and control link has the advantages of anti-jamming and anti-interception, and its complex electromagnetic environment, which also brings great difficulties to UAV detection. In this paper, the detection of civil UAV is realized by frequency hopping signal monitoring. Firstly, by analyzing the signal characteristics of UAVs, an adaptive noise threshold calculation method is proposed for find the signals from spectrum data. Then, the improved clustering analysis algorithm is proposed based on constructed the waveform shape characteristics and peak characteristics of UAV frequency hopping signal. Finally, according to the designed experimental process, the experimental environment is set up, and the UAV monitoring, discovery and parameter estimation are realized by using the improved clustering analysis algorithm, and compared with K-means, K-means^{++}, DBSCAN, Multi-hop and Auto-correlation methods. The results show that the method has certain robustness and has a good application prospect.

INDEX TERMS Civil UAV, hopping signal detection, clustering.

I. INTRODUCTION

Unmanned aerial vehicles (UAVs) of civil applications is growing rapidly across many application domains and improving ones' quality of life, such as real-time monitoring, providing wireless coverage, remote sensing, search and rescue, delivery of goods, security and surveillance, precision agriculture, and civil infrastructure inspection, up till now, UAVs industry has greatly promoted social and economic development, and become thousands of billions market value [1]–[3]. Meanwhile, civil UAVs are also faced many challenges within specific vertical domains and across many application domains, such as UAVs amateurs have weak air safety awareness, immature operation and imperfect air control system, and "illegal flying" of civil UAVs have brought unprecedented threats to aviation safety and personal

The associate editor coordinating the review of this manuscript and approving it for publication was Jing Liang[ID].

privacy [4]. To overcome these challenges, formulating relevant laws, regulations and policies to implement the supervision of UAVs must be done by the government, as well as technicalities of detecting, locating and controlling UAVs are urgently developed [5].

In existing studies, UAV detection methods mainly include sound monitoring, visible light, infrared or radar detection and radio spectrum monitoring, etc. [3]. Among them, sound monitoring is susceptible to the noise of surrounding life, visible light is usually affected by weather and building occlusion. While UAV miniaturization and even "invisible", makes infrared and radar detection technology difficult to play an advantage. Radio spectrum monitoring is through equipment (radio receiver and antenna, etc.) to monitor the UAV frequency band all-weather, analyze the spectrum data, then detect the control signal or the communication signal. Compared with these methods, spectrum monitoring has the advantages of good applicability and less influence by

the environment, become an important method for UAV discovery [6]–[10], [28].

The electromagnetic environment of UAV in radio frequency band is complex, noise and interference coexist [11], and most of the UAV signals are frequency hopping (FH) signals, which further increases the difficulty of detection and analysis. Research on FH signal detection, separation and recognition based on spectrum monitoring data has become a hot spot in UAV signal analysis field [12]–[15]. FH signal detection methods are mainly frequency domain and time domain detection. Common frequency domain analysis methods include Fourier transform [16], wavelet analysis [17], [18], Wigner-Ville distribution [19], spectrogram, etc. [20]–[22]. Time domain detection methods include image analysis, energy detection, correlation detection, etc. [23]–[28].

The paper in [14] propose an improved channelized MWC scheme for non-cooperative detection and frequency estimation of FHSS signals, by adjusting the channel weighting factor, it can better adapt to the single hop width, greatly reduce the amount of calculation, and achieve good results compared to the traditional method, but only based on theoretical analysis and numerical simulations, and not real implementation of channelized MWC. In [15], [16], [19] papers, a novel method based on sparse linear regression to solve the problem of computation burden in parameters estimate, which the results are only better on hop timing estimation, the estimation performance of other parameters is general. An approach based on frequency difference and one-dimensional non-linear filter has been proposed in [18], which the robustness against white Gaussian noise has been enhanced but need SNR is greater than 13 dB which is an extremely harsh precondition, and is also reflected in [20], the author propose a detection scheme based on the Neyman-Pearson test, and the results shows better than method of auto-correlation-based when the hopping period is short, and so on. the front papers methods almost set a harsh precondition, or manual parameter, and also not make a real environment experiment within multiple frequency hopping signals active, lacking of persuasion of practical application.

In this paper, by focusing on frequency characteristics of the civil UAV control link signals (which are FH signals), a new FH signal detection of civil UAVs based on improved K-means clustering algorithm is proposed to fast discovery civil UAVs. Concretely, an adaptive noise threshold calculation method is firstly provided to preprocess spectrum data of civil UAVs in radio frequency band. Then an improved K-means clustering algorithm is proposed to analyze FH signals of civil UAVs and estimate parameters of them. Experiment results and comparison with K-means, K-means^{++}, DBSCAN, Multi-hop and Auto-correlation methods finally show that the proposed method is useful and effective to detect civil UAVs.

The rest of this paper is structured as follows: In Section II-A, characteristics of frequency hopping signals of civil UAVs are briefly reviewed. In Section II-B,

introduce the idea of frequency hopping signal detection of the paper. In Section III, the process of the method to detect FH signals of civil UAVs is described in detail. In Section IV, several experiments are built to verify the performance of the proposed algorithm. In Section V, the performance of the algorithm is compared and analyzed, and conclude the paper is in Section VI to show.

II. FREQUENCY CHARACTERISTICS AND DETECTION OF CIVIL UAV CONTROL LINK SIGNALS

FH signals of civil UAVs work in open ISM band 2400MHz-2483.5MHz, in which there are WIFI, wireless mouse, cord-less phone, blue-tooth, microwave and ZigBee besides FH signals of UAVs [11], hence electromagnetic environment is often very complex, such as Figure 1 shows the spectrum waterfall map for electromagnetic environment of UAVs in ISM band at some time.
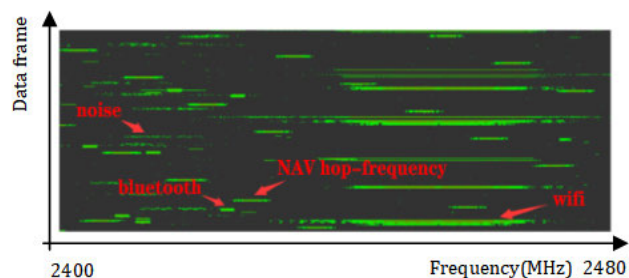

FIGURE 1. The spectrum waterfall map for electromagnetic environment of UAVs.

In the section, frequency characteristics and detection of FH signals of civil UAVs are analyzed.

A. FREQUENCY CHARACTERISTICS OF FH SIGNALS

Comparison with other signals in the ISM band, FH signals of civil UAVs own many interesting and important characteristics, which can help us to parameterize the FH signals not only from the theoretics but also applications point of view [11], [16], [22], [28]–[32]. In the paper, as Figure 2 shows, these characteristics are summarized as follows:
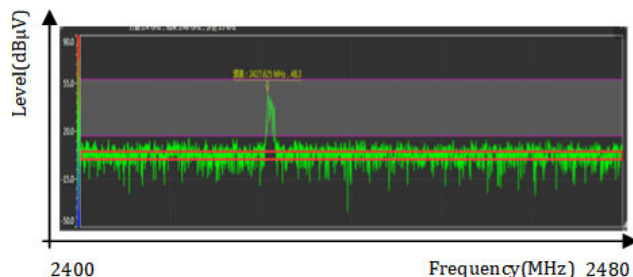

FIGURE 2. A frame of spectrum data of UAV.

The bandwidth of the FH signal of a civil UAV is stable. The bandwidth of a FH signal is consisted by the transmission bandwidth and the protection bandwidth. The former is the distance between the maximum and minimum frequency points of the FH signal, which is theoretically about 2MHz; the latter is to protect the effective transmission of

a FH signal. In most real applications, 1MHz protection bandwidth is added to the left and right of the FH signal respectively, hence the bandwidth of an actual received civil UAV signal is about 4MHz.

The frequency sequence of a civil UAV FH signals is fixed. The frequency sequence is a set of non-repetitive chronological frequency points of an actual received civil UAV signal. And in real applications, the FH frequency sequence of a civil UAV signal is often unchanged.

FH signals law of civil UAV can be observed. Despite the dwell time of the signals is very short between two FH in a certain span (it is usually microseconds), the FH period of the civil UAV signal is fixed, i.e., the sum of the time that the signal energy starts to disappear and the next FH energy starts to rise is fixed. In addition, FH speed (the rate of the frequency hops and time) and peak energy of a civil UAV signal are stable, the signal of 100-1000 hops per second is medium speed FH signal.

Theoretically, the aforementioned frequency characteristics can be utilized to distinguish FH signals of civil UAVs from signals in open ISM band 2400MHz-2483.5MHz. However, obtaining these frequency characteristics are not trivial. In real world applications, special data mining methods are needed to extract these frequency characteristics of FH signals of civil UAVs.

It is worth noting that there are Bluetooth signals almost have some same characteristics, such as frequency hopping, active in 2400MHz-2483MHz, frequency hopping time-sequence, and a stabled dwell time, the difference is that Bluetooth signals is only 1M bandwidth in real applications, and transmission distance is less than 30 meters, and even if in an open environment, the transmission distance is less than 60 meters, which is within sight. Therefore, we can combine the actual environment and frequency hopping signal detection results for comprehensive analysis to determine whether there are Bluetooth signals.

B. DETECTING FH SIGNALS OF CIVIL UAVS

From the data mining point of view, based on frequency characteristics of a FH signal of a civil UAV, the FH signal can be parameterized, i.e., the FH signal can be expressed into frequency characteristics space, and then the civil UAV can be discovered by detecting the FH signal in the frequency characteristics space. In this paper, bandwidth, waveform, short-time peak energy and time sequence features are selected as frequency characteristics of FH signals, furthermore to extract four frequency characteristics of signals, an improved K-means clustering algorithm are proposed to classify signals in open ISM band according to each frequency characteristic, respectively. Then FH signals are detected according to clustering results of four frequency characteristics of signals. Intuitively, Figure 3 shows dwell time, bandwidth, cycle and interval of FH signals of civil UAVs.

In addition, because there exists noise in any radio signals, an adaptive noise threshold calculation method is provided
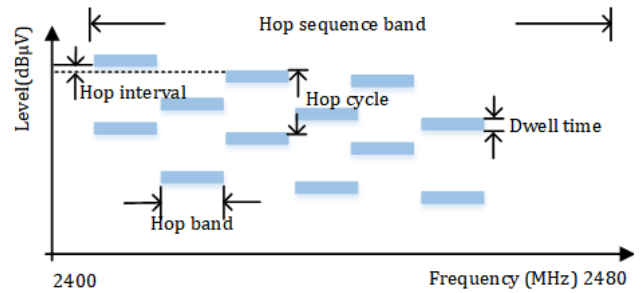

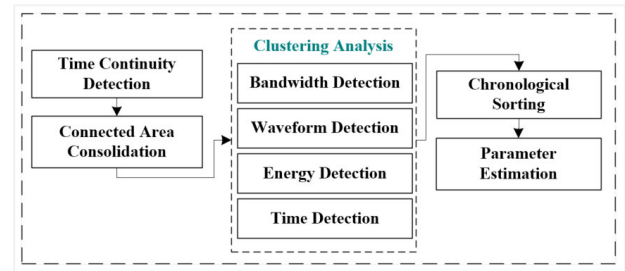**FIGURE 3.** The schematic chart of FH signal parameters.

FIGURE 4. Detection of FH signal of UAV process.

to preprocess signals. From the data analysis point of view, the adaptive noise threshold calculation method is mainly used to extract the spectrum data higher than the noise threshold, the process is equal to obtain effective spectrum data of radio signals.

From these ideas, the FH signal of UAV is detected from the characteristics of signal duration continuity, signal frequency point connectivity, bandwidth similarity, waveform feature similarity, short-time peak energy similarity and time sequence correlation. Specifically, aiming at FH signal detection in low SNR electromagnetic environment, according to the characteristics of noise and signal distribution in frequency domain, the adaptive noise threshold calculation method is used to extract the spectrum data higher than the noise threshold. Then, the improved clustering algorithm is used to cluster the extracted signals with bandwidth, waveform, energy and dwell time characteristics to detection the FH signals of UAV, and estimate the parameters. The schematic chart is shown in Figure 3, and the algorithm processing is proposed is shown in Figure 4, which shows the process of using improved clustering algorithm to detect and sorting the FH signal of UAV in detail, and analyzes the system error at the end of experiment:

1) The FH signal of UAV is extracted by adaptive threshold calculation method.

2) Using the improved clustering algorithm to extract the signal bandwidth, wave form characteristics and resident time, energy, then clustering.

3) Separation of various classification according to the time sequence, the class whose number of signals in the sorting results is less than 10% of the total number of detected signals is discarded;

4) The FH signal parameters of the classification results are estimated.

III. THE PROPOSED METHOD TO DETECT FH SIGNALS OF CIVIL UAVS

According to *ITU-R P372 proposal*, radio noise obeys the normal distribution under certain conditions, theoretically, this also means that the number of noise points in the spectrum distribution is more than the number of signal points, and with the accumulation of time, the statistical distribution characteristics of signal and noise become more obvious. Intuitively, noise points and signal points in frames of spectrum data are convex distribution, which are shown in Figure 5, where θ is the signal threshold.
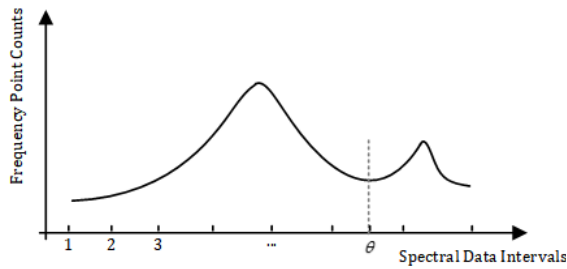
FIGURE 5. Schematic diagram of spectral data distribution.

A. ADAPTIVE THRESHOLD CALCULATION METHOD

Up till now, there are many researches for how to obtain signal threshold θ [23]–[25]. In [23], an automatic algorithm extraction of the signal components (useful information) from the noisy mixture is based on the time-frequency distribution segment to a fixed number of data classes is proposed, which depends on the differences in the time frequency structures of noise and signal components. In [24] paper innovatively proposed a dynamic threshold based target signal cooperative extraction method for high frequency electromagnetic environment measurement, which reduces the influence of manual factors and improves the automatic degree and efficiency of high frequency electro-magnetic environment measurement, but it's not completely applicable to detect uav signals which is in a moving status and complex frequency environment.

In the paper, inspired by the characteristics of the FH signal of UAV, the adaptive threshold calculation method based on current spectrum data is proposed. Formally, let a frame of spectrum data in open ISM band $S_t = \{s_1, s_2, \cdots, s_n\}$ (where s_i is signal energy level (dbμV) of i sampling point), then the signal level interval of the spectrum data can be calculated, i.e., $[S_{min}, S_{max}]$ in which $S_{min} = min\{s_1, s_2, \cdots, s_n\}$, $S_{max} = max\{s_1, s_2, \cdots, s_n\}$. Suppose split width of interval is b, for example, $b = 2db\mu v$ in real applications, then the level interval $[S_{min}, S_{max}]$ can be divided by $m = \frac{S_{max} - S_{min}}{b}$ sub-intervals, denoted by $[S_{min-1}, S_1], [S_1, S_2], \cdots, [S_{m-1}, S_m = (S_{max})]$ such that $S_j = S_{j-1} + b$ for each $j \in \{2, \cdots, m\}$. According to m sub-intervals, statistical analysis of the FH signal can be finished in the frame of spectrum data, then the number of sampling points in each sub-interval can be obtained, i.e., $S_i \in [S_{j-1}, S_j]$. Accordingly, statistical law of the FH signal
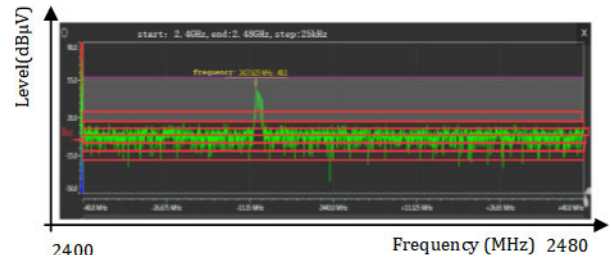
FIGURE 6. Energy segmentation diagram of a frame of spectrum data.

can be described by the following function:

$$y = F(x),$$

where $x \in \{[S_{min-1}, S_1], [S_1, S_2], \cdots, [S_{m-1}, S_m = (S_{max})]\}$, y is the number of sampling points in x. Based on frequency characteristics and our experiment on FH signals of UAV, the function can be shown in Figure 6, and signal threshold θ can be obtain in the function, i.e., θ is the minimum of the function. Algorithm 1 can be designed to obtain threshold θ of FH signals of UAV.

Algorithm 1 Obtaining Threshold θ of FH Signals UAV
Input: Spectrum data in open ISM band
Output: Threshold θ
1)   let a frame of spectrum data: $S_t = \{s_1, s_2, \cdots, s_n\}$, level scope: $[S_{min}, S_{max}]$.
2) $m = \frac{S_{max} - S_{min}}{2}$ sub-intervals denote as $S_i = \{[S_{min}, S_1], [S_1, S_2], [S_2, S_3], \cdots, [S_{m-1}, S_m(= S_{max})]\}$.
3)   for $[S_k, S_{k+1}]$ in S_i do
4)   Count sampling points as C_k,
5)   if $k == 0$ or $C_{max} < C_k$
6) $C_{max} = C_k$;
7) $q = k$;
8)   end
9)   for $[S_q, S_{q+1}]$ in S_i do
10)   Count sampling points as C_q,
11)   if $C_{q-2} > C_{q-1} > C_q < C_{q+1} < C_{q+2}$
12) $C_{min} = C_q$;
13) $\theta = S_{q+1}$;
14)   break;
15) end
16) return θ

Signal extraction: spectrum signals, and uav signals in special have the statistical characteristics of spectrum data as shown in the figure 5, except signals submerged in the noise, we can get a better adaptive threshold θ by Algorithm in a lower SNR environment, then the spectrum data is reprocessed based on this threshold, and signals list is obtained, then cluster analysis algorithm is carried out.

B. AN IMPROVED K-MEANS CLUSTERING ALGORITHM

Unlike the traditional K-means algorithm, in which the number of clusters need to be fixed and initial clustering centers

are randomly selected, in this paper, an improved K-means clustering algorithm is proposed, in which the number of clusters are decided by density characterization of objects and clustering centers are selected as objects with maximum density.

Step 1: Given m data objects $\Omega = \{o_1, o_2, \cdots, o_m\}$, in which $o_i = (a_{i1}, a_{i2}, \cdots, a_{in})$, $i = 1, 2, \cdots, m$, n is the attribute dimension of the data, the Euclidean distance of any two objects o_i and o_j is as follows:

$$d_{ij}(o_i, o_j) = ||o_i - o_j|| = \sqrt{\sum_{q=1}^{n} (a_{iq} - a_{jq})^2} \quad (1)$$

For object o_i, denote the following distances:

$$d_{i\min} = \min\{d_{ij}|j \in \{1, 2, 3, \cdots, m\}, j \neq i\} \quad (2)$$
$$d_1 = \min\{d_{i\min}|i \in \{1, 2, 3, \cdots, m\}\} \quad (3)$$
$$d_2 = \max\{d_{i\min}|i \in \{1, 2, 3, \cdots, m\}\} \quad (4)$$

Intuitively, $d_{i\min}$ is the minimum distance from all objects $o_j (j \neq i)$ to object o_i, d_1 and d_2 are the minimum and maximum values of $\{d_{i\min}|i \in \{1, 2, \cdots, m\}\}$. Based on d_1 and d_2, the clustering radius R is calculated as follows:

$$R = w \times d_1 + (1 - w) \times d_2, \quad w \in [0, 1] \quad (5)$$

in which $w \in [0, 1]$, if $w = 1$, then $R = d_1$, it means that each object of Ω is a cluster. If $w = 0$, then $R = d_2$, it means that there is at least a cluster with only one object. In real world applications, w is often in $(0, 1)$. Obviously, the clustering radius R directly affects the result of data classification. The smaller clustering radius R is, the fewer number of elements in each cluster will be, and the greater number of clusters is. The result of rough clustering and excessive clustering is unreasonable. Therefore, we need to analyze the actual data characteristics and the distribution characteristics of the data, then select a suitable weight w and obtain the clustering results, in this paper, take $w = 0.5$, which get a better signal detect accuracy performance in experiment environment as shown in Figure 7.
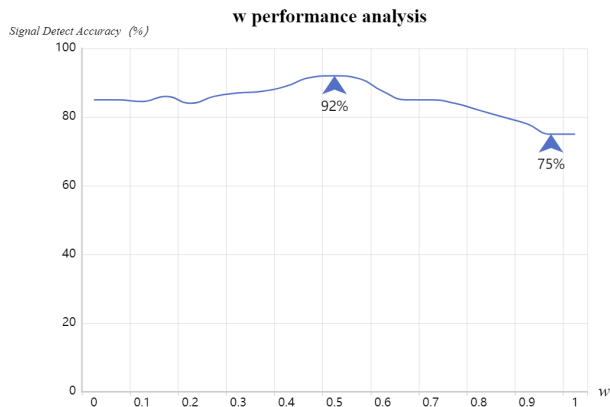

FIGURE 7. *w* performance analysis in experiments.

In Figure 7, w performance in experiments is trend to be stable above 80% when the value is less than 0.9, more than 0.9 decline to 75%, which may be related to the current

density of spectrum data of itself, and get the best signal detect accuracy about 0.5 reach 92%.

Step 2: Calculate the density of every object in Ω according to the clustering radius R. Formally, the density of objects o_i is calculated by c_1.

Step 3: clustering centers and Clustering results. Formally,
1) The first clustering center c_1 is selected according to the maximum density, *i.e.*, $c_1 = o_l$ if o_l is such that

$$\rho_l = \max\{\rho_j|j = 1, 2, \cdots, m\}$$

the cluster $C_1 = \{o_j|||o_j - o_l|| \leq R, j = 1, 2, \cdots m\}$.
2) Suppose k-*th* clustering center c_k and k-*th* cluster C_k are selected.
3) Then (k+1)-*th* clustering center c_{k+1} and (k+1)-*th* cluster C_{k+1} are $C_{k+1} = o_{l'}$, if $o_{l'}$ is such that

$$\rho_{l'} = \max\{\rho_j|o_j \in \Omega - \cup_{k'=1}^{k} C_{k'}\}$$
$$C_{k+1} = \{o_j|||o_j - o_{l'}|| \leq R, o_j \in \Omega - \cup_{k'=1}^{k} C_{k'}\}$$

Step 4: In addition to all the element objects that have been classified, repeat the above steps for the remaining data until all the data element objects are classified.

IV. EXPERIMENTAL VERIFICATION
A. EXPERIMENTAL ENVIRONMENT
In the experiments, three different of UAVs and their remote controllers: UAV-A: DJI/PHANTOM/4/PRO/v2.0 (2.4GHz, FH), UAV-B: DJI/MAVIC/AIR (5.8 GHz, constant frequency, 2.4G, FH), UAV-C: DJI/MATRICE/600/PRO (2.4G, FH), ZX219 radio receiver (20MHz-8GHz) and antenna TN341 (20MHz-6GHz) are used to collect data in an opening environment., which are shown in Figure 8.

（a）DJI PHANTOM 4 PRO V2.0   （b）DJI MAVIC AIR

（c）DJI MATRICE 600 PRO   （d）Antenna and Receiver

FIGURE 8. Experimental equipment and devices.

B. EXPERIMENTAL PROCESS

1) CALCULATION OF ADAPTIVE THRESHOLD

1) Calculate the maximum level $L_{\max}$ and minimum level $L_{\min}$ of the spectrum data frame. The level values are segmented by $2dB\mu V$ in interval $[L_{\min}, L_{\max}]$, the continuous $d_k \in D, k = 1, 2, \cdots m$ frames data are segmented in turn. The number of data points of d_k in each segment is counted as $\{c_{k1}, c_{k2}, \cdots, c_{kp}\}$ respectively, where p is the total number of segments d_k, and the segment of the maximum number of data points is obtained;

2) Find the θ position in the interval obtained in step 1) as shown in Figure 5. If the number of data points in the interval is continuously less than the number of points in the two adjacent intervals, the upper boundary value of the interval is the signal threshold of the current frame data.
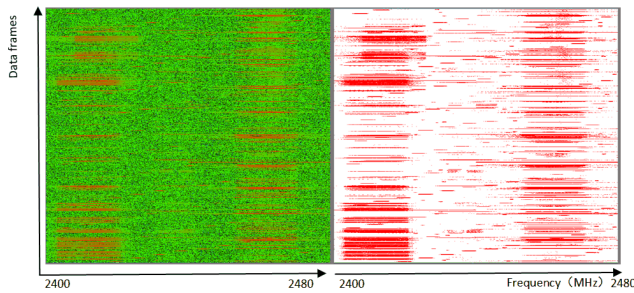

FIGURE 9. Spectrum waterfall map after threshold processing.

As shown in Figure 9, it is a waterfall map of 1442 frames of spectrum, in which the left is the original spectrum and the right is the spectrum data of extracted signals through threshold processing and noise be cleared. The signal frequency band is 2.4GHz-2.48GHz, and the sampling time is 1s. The color changes from red RGB (255,0,0) to green RGB (0,255,0), corresponding to the maximum and minimum level value range of 1442 frames.

For FH signal detection of UAV, generally, the electromagnetic environment in a short time period will not change too much, then the initial threshold value can be used as the signal judgment for the monitoring process.

2) A SINGLE FREQUENCY SIGNAL DETECTION

1) The threshold is used to compare the level of the spectrum frame by frame. When the level is greater than the threshold, indicate signal present, otherwise no signal.

2) Continuously compare the data frame of the current frequency. When the signal exists continuously, count the start time and end time of the signal: the start time is the first time that the frequency point level is greater than the threshold, and the level first time less than the threshold as the end time of the signal after appears continuously. Denote the signal of this frequency point as s_i.

3) When processing data at the last frame of the sampled data and the signal of the current frequency point still exists, the signal is discarded directly which purpose is to avoid parameter estimation error.

TABLE 1. The signal detection schematic.

	f1	f2	f3	f4	f5	...	f3200
t1	0	0	0	0	1	...	0
t2	0	1	0	1	0	...	0
t3	1	1	0	1	0	...	0
t4	1	1	0	1	0	...	0
t5	1	1	1	1	0	...	1
t6	0	1	1	1	0	...	1
t7	1	0	1	0	0	...	1
t8	0	1	1	1	0	...	1
t9	0	0	0	0	0	...	0
t10	0	1	0	0	0	...	1
t11	0	0	0	1	1	...	0
t12	0	0	1	1	1	...	0
t13	0	1	1	1	0	...	0
t14	0	0	0	0	0	...	0
...	...	...	...	...	...	...	1
t10000	0	1	0	0	1	...	1

The signal information of a single frequency expressed as $S_i = \{S_1, S_2, \cdots, S_n\}$ is shown in Table 1. The data filled with a blue background show that the frequency point level is greater than the threshold at the corresponding time. Each row represents a frame of data. Columns f_i(MHz) indicates whether the frequency point presence signal at different times, 1 is present, and 0 indicates disappear. Frequency f_i can calculated by subject: $f_i = 2400 + i \times 0.025$, of which i is serial number of f_i.

3) TIME CONTINUITY DETECTION

In general, the single-hop FH signal has a certain dwell time. Intuitively expressed as at least two consecutive frames of spectrum data. For 10000 values at each frequency point, we eliminate these abnormal values whose current value is 1 and its adjacent values are 0. And the signal frame is eliminated which the end time is the last frame of sampling data. This method of time continuity detection can eliminate noise or interference to a large extent, but the low SNR signal is not eliminated. For the data in Table 1, to be eliminated is shown in the gray background, and the blue background is the reserved signal after elimination, as shown in Table 2.

TABLE 2. Elimination noise interference data.

	f1	f2	f3	f4	f5	...	f3200
t1	0	0	0	0	1	...	0
t2	0	1	0	1	0	...	0
t3	1	1	0	1	0	...	0
t4	1	1	0	1	0	...	0
t5	1	1	1	1	0	...	1
t6	0	1	1	1	0	...	1
t7	1	0	1	0	0	...	1
t8	0	1	1	1	0	...	1
t9	0	0	0	0	0	...	0
t10	0	1	0	0	0	...	1
t11	0	0	0	1	1	...	0
t12	0	0	1	1	1	...	0
t13	0	1	1	1	0	...	0
t14	0	0	0	0	0	...	0
...	...	...	...	...	...	...	1
t10000	0	1	0	0	1	...	1

The waterfall map of spectrum and after eliminating noise is shown in Figure 10, with the same color mark as above.
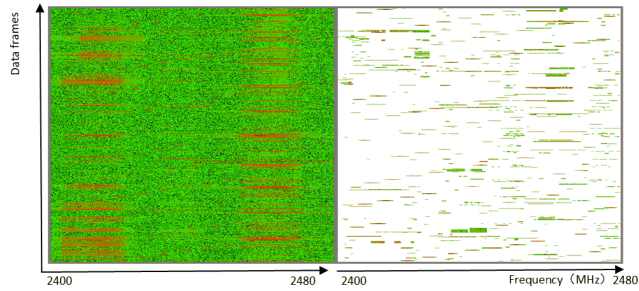

FIGURE 10. Noise and interference processing.

4) MERGE OF CONNECTED REGION

For $S = \{S_1, S_2, S_3, \cdots, S_i, \cdots, S_{3200}\}$, from S_1 to S_k, $k \in [1, 3200]$, judge whether signals S_k and S_{k+1} are overlapping in their time intervals $[t_1, t_2]_{S_k}$ and $[t_1, t_2]_{S_{k+1}}$ in turn. If so, merge the two signals in the way of maximizing the time gap between starting and ending. As shown in Table 3, all signals in each frequency point are combined, including two connected regions: the first connected region is a signal with dwell time of $[t_2, t_8]$ and frequency of $[f_1, f_4]$, the second connected region is another signal with dwell time of $[t_{11}, t_{13}]$ and frequency of $[f_3, f_5]$. All the connected regions constitute a set of signals: Ω.

TABLE 3. The connected regions after merging.

	f1	f2	f3	f4	f5	...	f3200
t1	0	0	0	0	1	...	0
t2	0	1	0	1	0	...	0
t3	1	1	0	1	0	...	0
t4	1	1	0	1	0	...	0
t5	1	1	1	1	0	...	1
t6	0	1	1	1	0	...	1
t7	1	0	1	0	0	...	1
t8	0	1	1	1	0	...	1
t9	0	0	0	0	0	...	0
t10	0	1	0	0	0	...	1
t11	0	0	0	1	1	...	0
t12	0	0	1	1	1	...	0
t13	0	1	1	1	0	...	0
t14	0	0	0	0	0	...	0
...	...	...	...	...	...	...	1
t10000	0	1	0	0	1	...	1

5) SIGNAL BANDWIDTH DETECTION

Signal bandwidth detection steps are as follows:

1) For each signal S' in the set Ω, Bandwidth $B = f_e - f_s$, f_s and f_e are the starting and ending frequencies of the S', respectively.

2) If the signal bandwidth is outside the range of 0.5 MHz-10MHz, the signal is discarded, and only the signal within the range of 0.5 MHz-10MHz is retained for further feature detection.

3) The improved clustering algorithm is used for clustering and sorting, and the signal bandwidth is taken as input data.

4) Discard the classification with less than 5 elements in the result of clustering.
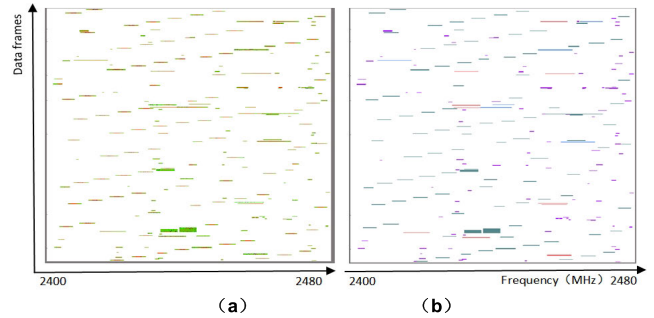

FIGURE 11. Detection and sorting with signal bandwidth.

Figure 11 shows the results of signal bandwidth clustering and sorting. The signal bandwidths are extremely close to the same category, and the signal bandwidth has a certain gap to the different categories. The signal bandwidth detection method can effectively divide the signal data of fixed bandwidth into one category, and different bandwidth into different categories. A total of 4 categories are obtained, as shown in Figure 12, all signals of the same category are marked by the same color.
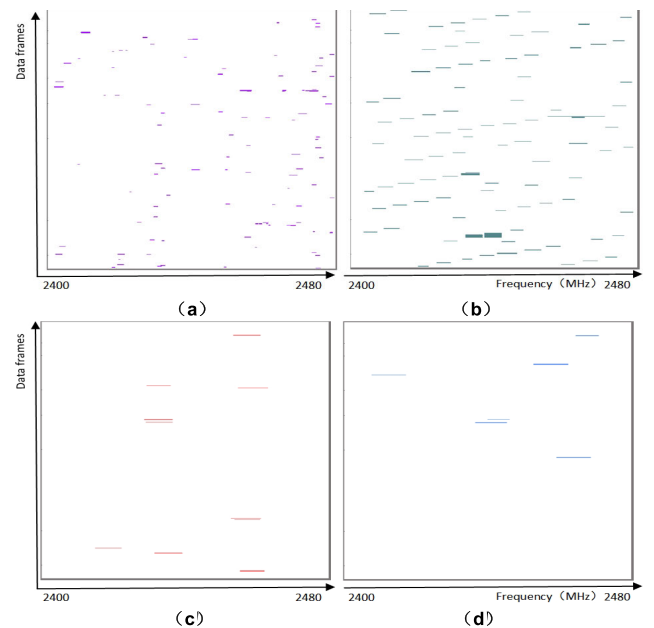

FIGURE 12. Classification based on signal bandwidth.

From Figure 12, we can see that the first category (a) has the largest number of data elements, in fact, the signal threshold is almost close to the base of the noise, so it contains short noises. Some signals in the second category (b) can be clearly seen appear regularly, that is, there are FH signals and some interference signals. The signals in the third classification

(c) have no obvious regularity, some may be burst signals, frequency hopping signals or noise data. A small number of signals in the fourth classification (d) may be signal or interference data. In subsequent clustering and parameter estimation, the classification (d) that does not have obvious FH signal characteristics and the number of elements in the category is less than 5 will be eliminated.

6) SIGNAL WAVEFORM DETECTION

The waveform characteristic value is calculated as follows:

1) $\forall S' \in \Omega$, Divide the bandwidth B of S' into 8 segments as $F_i = \{[f_s, f_1], [f_1, f_2], \cdots, [f_7, f_e]\}$.

2) Calculate the mean of level value in each segment in F_i one by one, get set $V_i = \{v_1, v_2, \cdots, v_8\}$, that is, the waveform characteristic value of the signal.

3) The improved clustering algorithm is used for input parameters of all categories of signals waveform, and the results are shown in Figure 13.
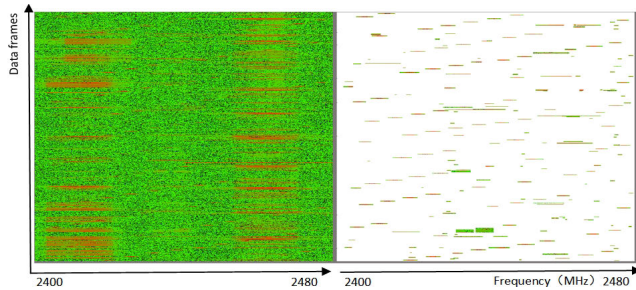
FIGURE 13. Process of signal waveform characteristics.

Specifically, for each category in Figure 13. Clustering detection result of class (a) in Figure 12 based on waveform similarity is shown in Figure 14(a1). The result of eliminating classes with elements lower than 5 is shown in Figure 14 (a2). Accordingly, the results of class (b-c) of clustering and results of eliminating the number of elements below the threshold are shown in Figure 14(b1-b2) and (c1-c2). After eliminating part of the interference, we can from the following figures intuitively find the signals in each class are further divided after some of the interference signals are eliminated. Class (c2) has no signal information after processing, and will not be processed later.

7) SIGNAL ENERGY DETECTION

Generally, during sampling, the peak energy of FH signals is relatively stable, and its energy value of is often larger in the central frequency of the signal. The further away from the central frequency of the signal, the overall trend of the level value decreases rapidly. The energy distribution diagram of FH signal is shown in Figure 15.

Signal energy detection steps are as follows:

1) $\forall S' \in \Omega$, let the starting frequency of S as f_s, the ending frequency of S as f_e, the center frequency f_c can be calculate by formula: $f_c = (f_e - f_s)/2$.

2) Calculate the center frequency of $[f_s, f_c]$, $[f_c, f_e]$ as f_1, f_2, respectively. In the same way, the center frequencies of
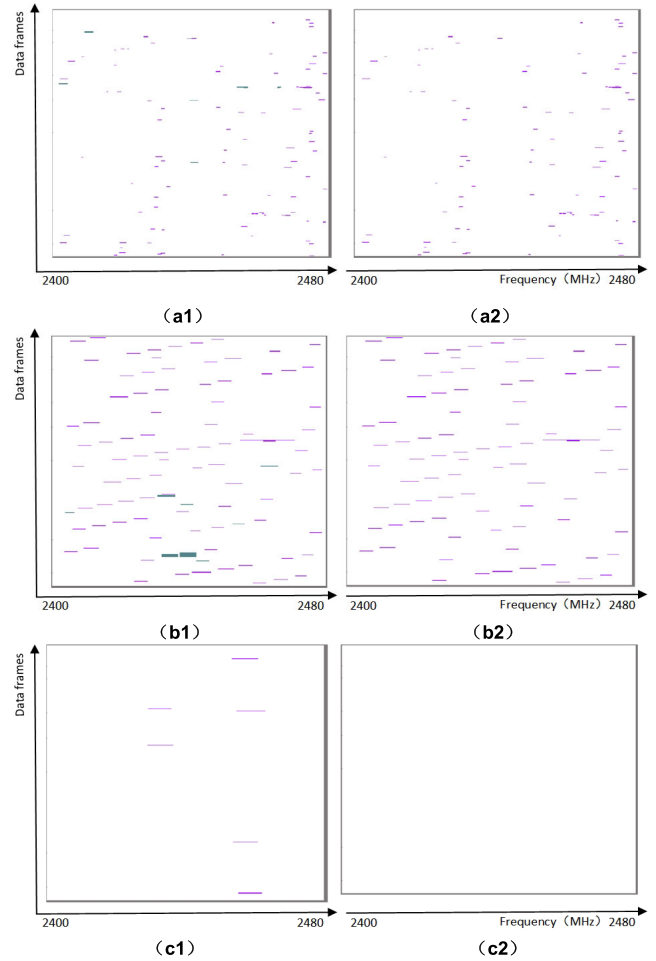
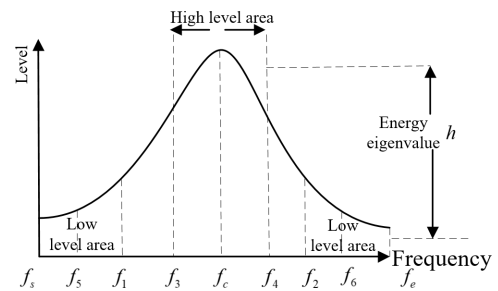**FIGURE 14.** Clustering based on waveform characteristics.

FIGURE 15. Schematic diagram of energy distribution of signal.

$[f_s, f_1], [f_1, f_c], [f_c, f_2]$ and $[f_2, f_e]$ are calculated as f_5, f_3, f_4, f_6, as shown in Figure 15.

3) According to the energy peak characteristics of frequency hopping signal, the interval $[f_3, f_4]$ is high-level value area, $[f_s, f_5]$ and $[f_6, f_e]$ are low-level areas, calculate the mean of level values in high-level area as l_{high}, the mean of level values in two low-level area as l_{low}, then the energy eigenvalue of signal is obtained by $h = l_{high} - l_{low}$.

4) Calculate the energy detection eigenvalues for all signals in Ω according to above steps, and get set $H = \{h_1, h_2, \cdots, h_k\}$.
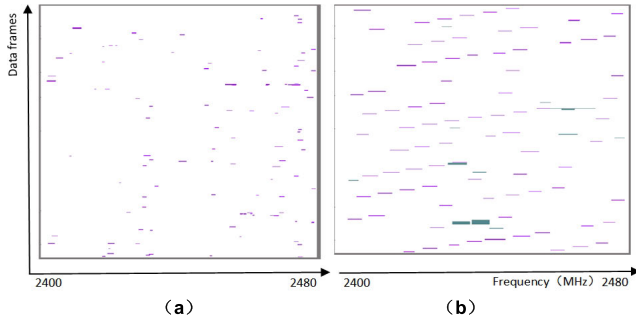
FIGURE 16. Clustering detection based on energy eigenvalues.

5) The characteristic value of signal energy is used as input parameter for clustering, and the results are shown in Figure 16, 16-(a) is correspond to Figure 14-(a2), Figure 16-(b) is refer to Figure 14-(b2).

8) SIGNAL DWELL TIME DETECTION

Signal dwell time detection steps are as follows:

1) $\forall S' \in \Omega$, set the starting time as t_s, the ending time as t_e, and calculate the dwell time $d = t_e - t_s$.

2) Calculate all signals in Ω according to the step 1), and get the signal dwell time set: $D = \{d_1, d_2, \cdots, d_k\}$, Diagram of signal dwell time is shown in Figure 17.
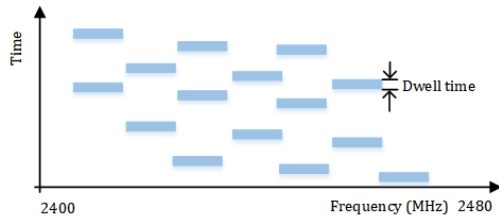

FIGURE 17. Schematic diagram of signal dwell time.

The results of dwell time clustering for the data processed after energy detection are shown in Figure 18. Three classes with the number of objects satisfying the condition are shown in Figure 19.

It can be seen from the diagram, the objects in their respective class (a), (b) and (c) are extremely similar. However, in the actual electromagnetic environment, there may be many FH signals of the same type of UAV at the same time. Therefore, it is necessary to classify the two types of hop signals according to the time sequence and the time gap stability characteristics.
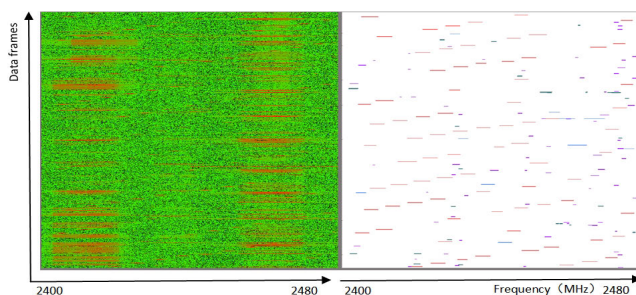

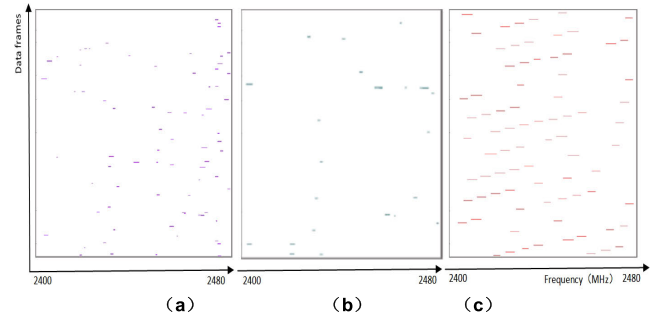**FIGURE 18.** Detection based on dwell time with clustering.

FIGURE 19. Clustering detection results based on dwell time.

9) CHRONOLOGICAL SORTING

The FH signals generated by UAV do not overlap in time series of each FH signal, so the possible situation in the detection environment is analyzed as follows:

1) If the time gap between all signals is stable or integer times of the minimum time period, there is only one UAV.

2) If multiple signals are crossed in time and spaced at a certain distance in frequency, two or more UAVs exist.

The characteristics of FH signal time sequence is shown in Figure 20, Frequency hopping signals with the same tag values (such as 1-7) but different background colors are overlapped in time.
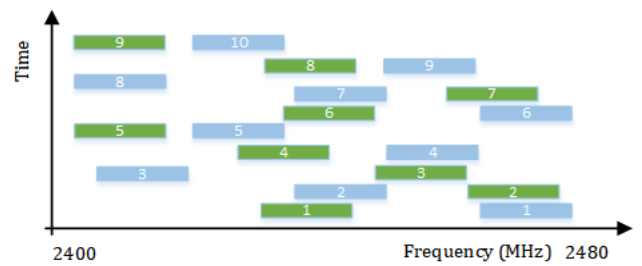

FIGURE 20. Schematic diagram of FH signal time sequence.

Specifically, the sorting operation steps of the time sequence characteristics are as follows:

1) Sort the signal objects in the order of their appearance at every category after clustering according to dwell time.

2) For each of the above categories, mark the original category as O. Divide the first element of O to a new category O', and taking out of element from O in turn, and judge whether it is continuous with the last element of O', if so, add it to the category O', else keeping forward judge whether
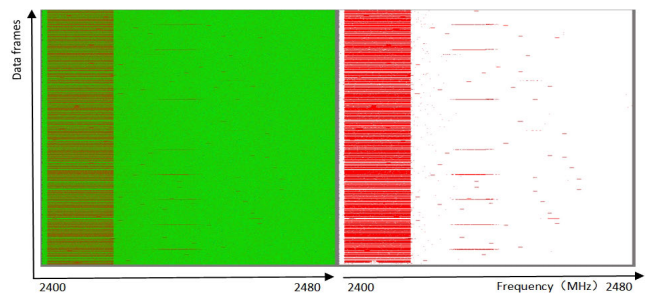

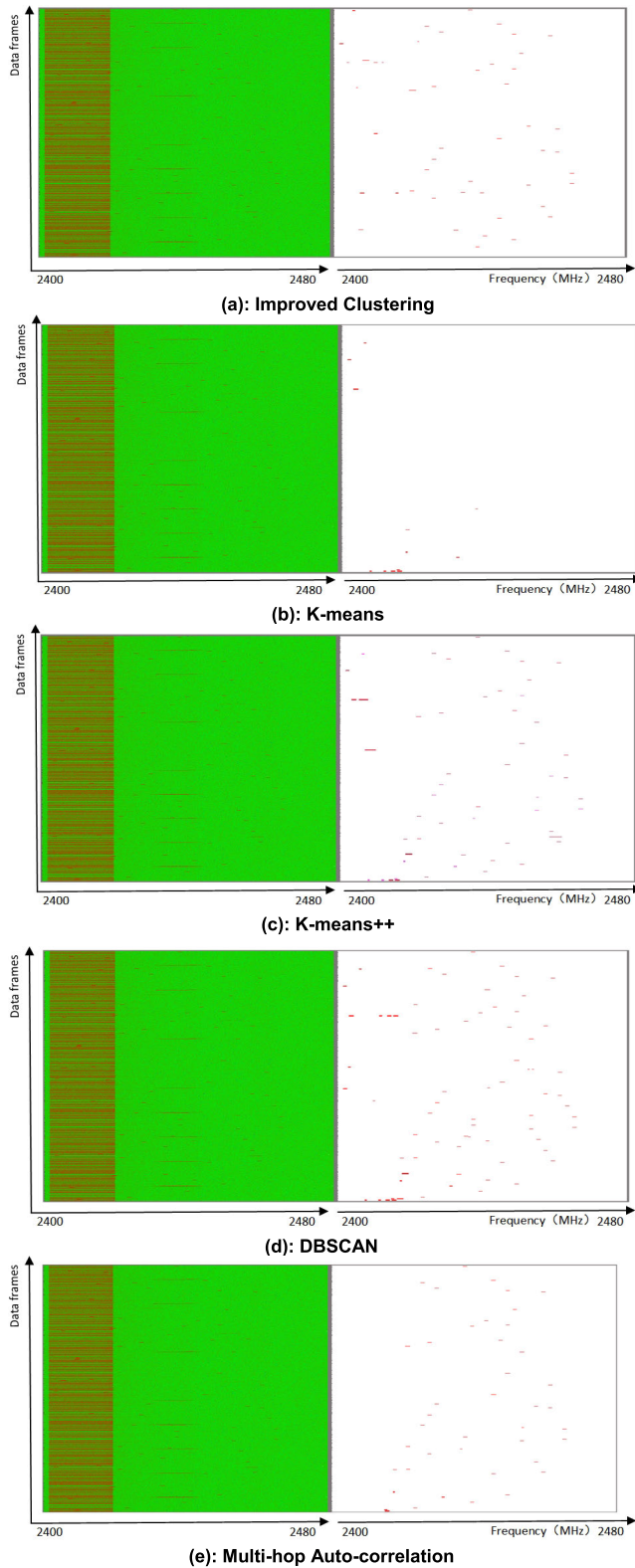**FIGURE 21.** Waterfall map after threshold processed of UAV-A signals.

(a): Improved Clustering

(b): K-means

(c): K-means++

(d): DBSCAN

(e): Multi-hop Auto-correlation

FIGURE 22. Detection results for UAV-A.

FIGURE 23. Waterfall map after threshold processed of UAV-B signals.

then set the first element of O' and the object to a new category O''.

3) Process all elements of O until each element is classified, and all signals in these categories do not overlap in time.

4) The categories in which the total number of elements less than 5 are eliminated, and the rest is the detection result of UAV FH signal.

In addition, two UAVs of the same model can be classified into a category, we can continue determine each category whether have two or more uavs by the common-sense knowledge which is that a single uav always can't appear two FH signals at a time, and then get the final results of uav FH signals detection.

C. EXPERIMENTAL RESULTS
The experiment in this paper mainly aims at the situation that there is only one UAV or two types of UAVs coexist. The proposed algorithm is applied to signal detection and verification, and the detection effect is compared with K-means and other methods.

1) ONLY UAV-A EXIST
Turn on the remote control of UAV-A, and use the radio receiver to scan the frequency band of 2.4GHz to monitor the signal. In the experiment, the spectrum (Figure 21, left) and processed signal (Figure 21, right) are presented by waterfall diagram. Different types of signals are distinguished by different colors, and the number of color types represents the number of UAVs. The waterfall map after threshold preprocessing of spectrum data is shown in Figure 21.

The processed results of the improved clustering algorithm, K-means (k = 2), K-means^{++}(k = 2), DBSCAN and Multi-hop Auto-correlation algorithm on frequency-sweep spectrum data of only existing UAV-A are shown in Figure 22. The results are shown in Figure 22(a-e), in which using K-means the algorithm doesn't detect the signal of UAV. Other methods all show that there is a UAV FH at least.

Through an in-depth analysis, the reason of K-means algorithm can't detect the signal is that the bandwidth (about 1MHz) of FH signal of this type of UAV is extremely close, which makes it unable to be divided into preset K(k = 2) categories. K-means^{++} method also has the problem of pre-set K(k = 2), but when selecting the initial cluster center, starting from the second cluster center, the object farthest from the first cluster center is selected as the candidate cluster

it is continuous with the other element of O', if continuous then make elements of O' from the first to current element to a new category O'', else continue to find forward, until the second element of O' is not continuous with the element,
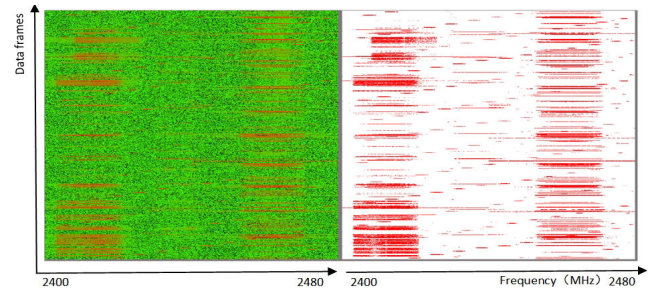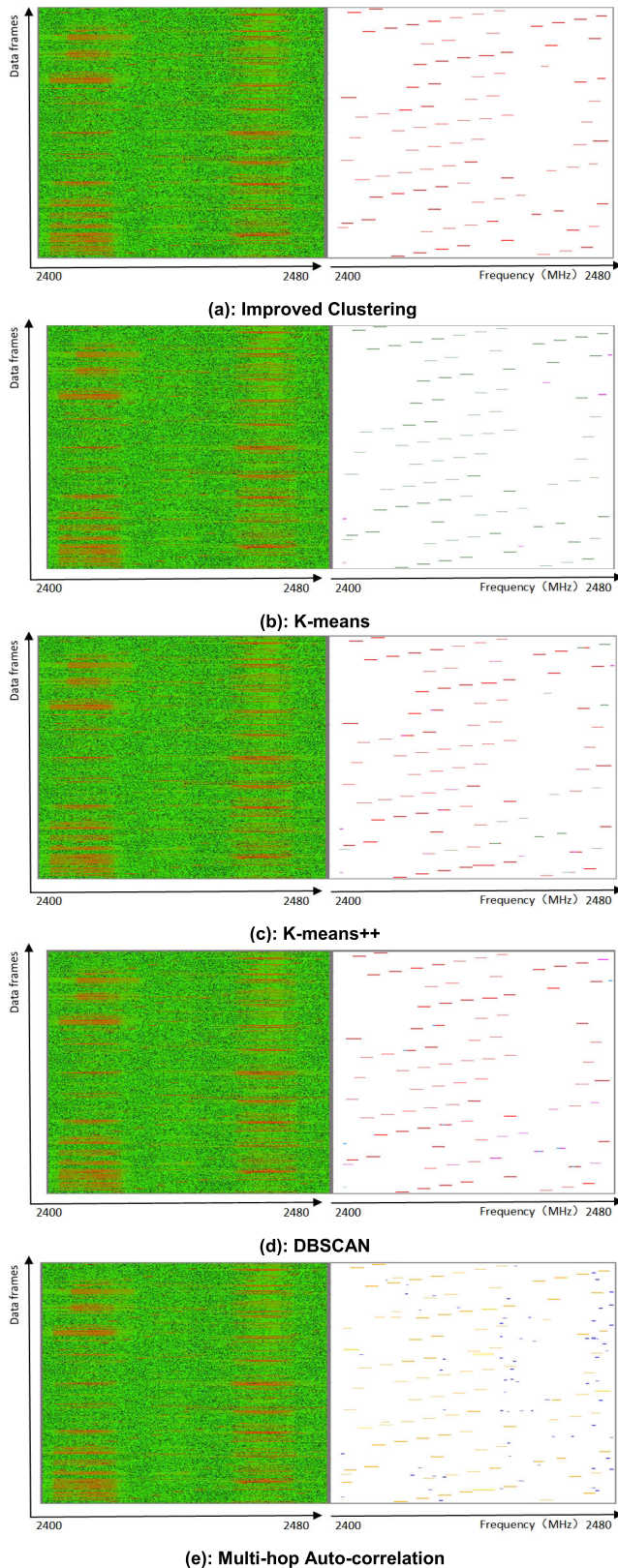
(a): Improved Clustering

(b): K-means

(c): K-means++

(d): DBSCAN

(e): Multi-hop Auto-correlation

FIGURE 24. Detection results for UAV-B.

center, that is, when the clustering elements are extremely close, at least one classification can be obtained, and the result is different from *K*-means.
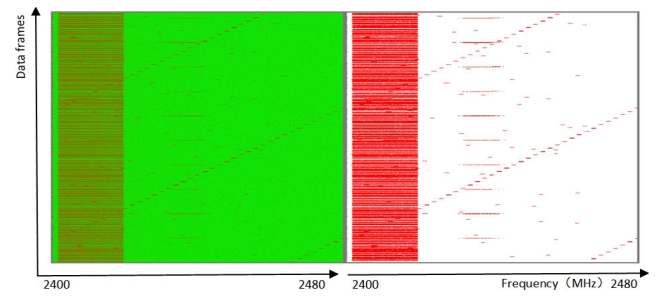

FIGURE 25. Spectrum waterfall after threshold processing.

2) ONLY UAV-B EXIST

Turn on the UAV-B remote control to test and verify only this UAV activity within the 2.4GHz frequency band. The spectrum data and the results after threshold processed of UAV-B signals are shown in Figure 23, the signal detection results shown in Figure 24.

As shown in Figure 24(a-e), the FH signal of UAV-B in current electromagnetic environment can be detected effectively by using improved clustering algorithm, and only one UAV signal be found. Although *K*-means (k = 2) algorithm can detect most FH signals, some interference signals cannot be removed in the classification results. Similarly, the detection results of *K*-means^{++} and DBSCAN algorithms contain some interference signals. The detection algorithm of Multi-hop Auto-correlation can retain all the undisturbed FH signals, but the detection results contain a large number of noise signals due to its strong correlation with unknown noise.

3) UAV-A AND UAV-C COEXISTENCE

In order to test the ability of these algorithms to detect FH signals of multiple UAVs, the remote controllers of two UAVs (A and C) are turned on at the same time. The spectrum data threshold preprocessing results are shown in Figure 25.

As shown in Figure 26 (a-e), different colors indicate the types of signals detected (*i.e.* the number of UAVs). Two types of FH signals are detected by improved clustering and Multi-hop Auto-correlation algorithm. *K*-means (k = 2) algorithm only detects one type of FH signal of UAV. Although *K*-means^{++} (k = 2) algorithm and DBSCAN detect two types of FH signals of UAV, a large number of noise and interference data need to be processed in the later parameter estimation stage.

V. EXPERIMENTAL ANALYSIS
A. ANALYSIS OF RESULTS
The UAV signals under different conditions are detected by improved clustering algorithm, *K*-means, *K*-means^{++}, DBSCAN and Multi-hop Auto-correlation. The number of detected UAV signals, the number of error detections, accuracy rate, error rate, running time and number of detected UAVs are shown in Table 4. Using the error detection rate and accuracy rate to analyze the performance of each algorithm under different experimental conditions, as shown in Figure 27 and Figure 28.
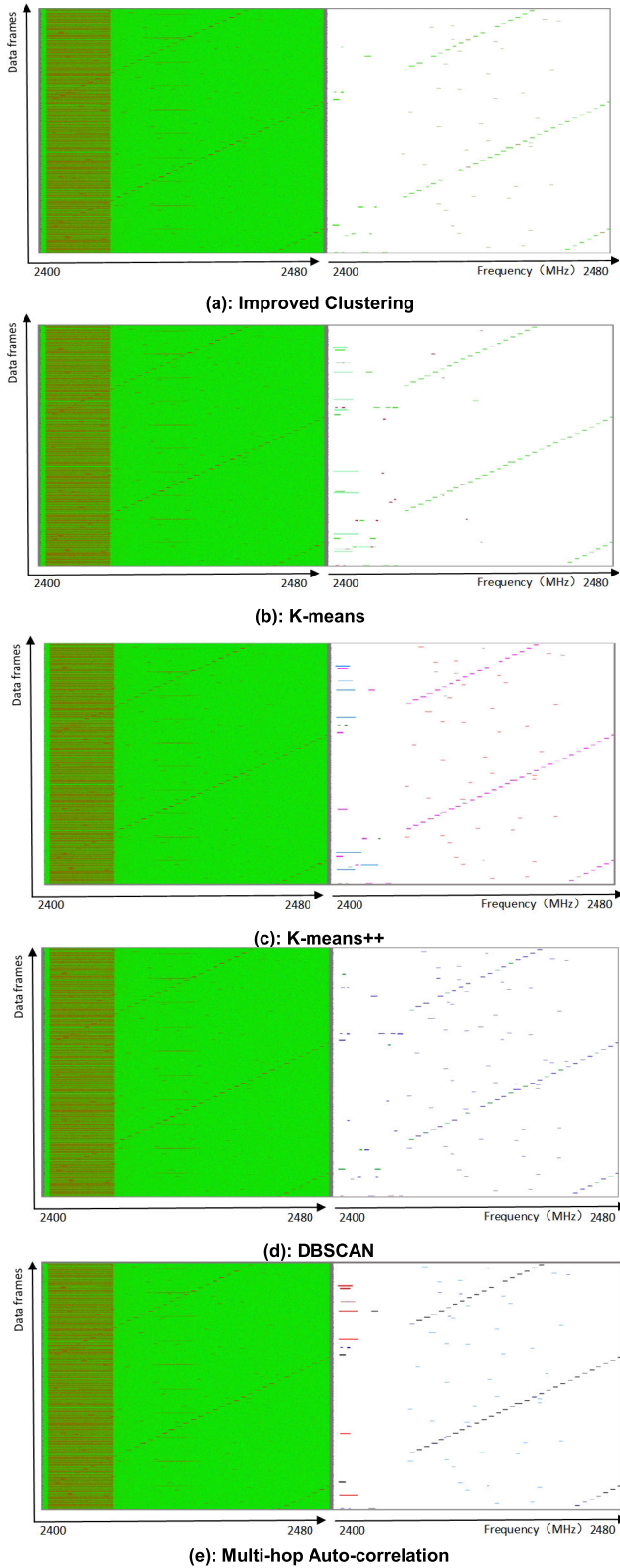
FIGURE 26. Detection results for UAV-A and UAV-C Coexistence.

TABLE 4. Experimental results of each algorithm under different experimental conditions.

| Experiment conditions		UAV-A	UAV-B	2 UAVs	
				UAV-A	UAV-C
	Number of FH signals	55	117	55	65
Improved Clustering	Number of signals	41	92	48	58
	False number of signals	2	1	2	6
	False detection rate	5%	1%	4%	10%
	Accuracy rate	68%	78%	84%	80%
	Running time(s)	0.01	0.06	0.04	
	Number of UAVs	1	1	2	
K-means	Number of signals	12	91	99	
	False number of signals	8	7	42	
	False detection rate	67%	7%	42%	
	Accuracy rate	7%	72%	48%	
	Running time(s)	0.01	0.02	0.39	
	Number of UAVs	0	1	1	
K-means++	Number of signals	54	99	37	61
	False number of signals	19	20	1	5
	False detection rate	35%	20%	3%	8%
	Accuracy rate	61%	68%	65%	85%
	Running time(s)	0.01	0.02	0.01	0.01
	Number of UAVs	1	1	1	1
DBSCAN	Number of signals	60	96	40	52
	False number of signals	15	12	1	11
	False detection rate	25%	13%	2%	21%
	Accuracy rate	79%	72%	71%	63%
	Running time(s)	0.04	0.04	0.02	0.02
	Number of UAV	1	1	1	1
Multi-hop Auto-correlation	Number of signals	42	101	33	52
	False number of signals	6	7	1	1
	False detection rate	14%	7%	3%	2%
	Accuracy rate	63%	80%	58%	78%
	Running time(s)	0.02	0.01	0.01	0.01
	Number of UAVs	1	2	1	1
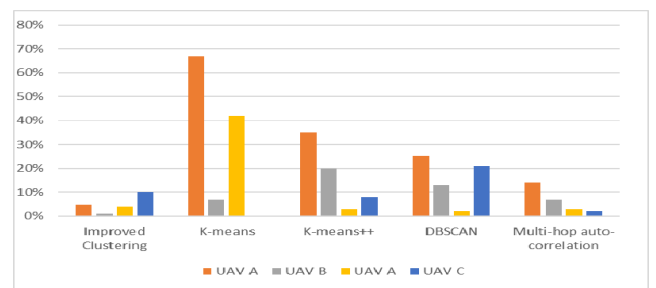
FIGURE 27. Comparison and analysis of error rate of detection.

that are not UAV FH signals. The accuracy rate is the proportion of the number of detected correct FH signals and the actual number of received FH signals. The error detection rate is the ratio between the number of non-UAV FH signals and the number of signals received from UAV. The running time is the total time from the beginning of algorithm running to the result output. The number of UAVs detected is the number of UAVs determined.

Basically, table 4 shows that algorithm of this paper has a lower error detection rate and accuracy performance
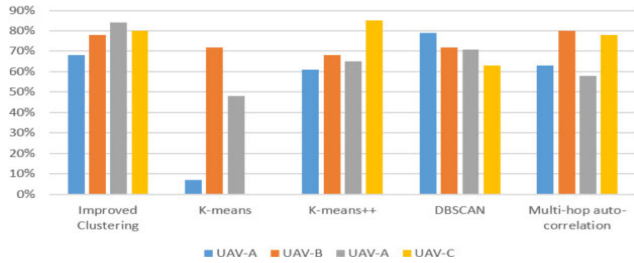
Among these algorithms, the number of detected signals is the number of UAV FH signals by each algorithm, the number of error detection signals is the number of detected signals

FIGURE 28. Comparison and analysis of accuracy of detection.

advantage when UAV-A FH signal activity only, the density-based DBSCAN clustering method has the highest accuracy, to some extent, it confirms that UAV FH signal has the advantage of density analysis, and on the contrary the traditional *K*-means method has a bad accuracy performance. On the one hand, the accuracy rate of the paper algorithm proposed in this paper is higher than most of the other four algorithms, whether there is only one FH signal activity of UAV-A or UAV-B, or when UAV-A and C coexist, indicating that the algorithm has certain stability, as shown in Figure 28. It has significant adaptability to detect UAV FH signals in different environments. On the other hand, the error detection rate of this algorithm is far lower than other algorithms in different cases, as shown in Figure 27, which improve the efficiency for further analysis and processing of UAV signals.

In short, through a variety of different tests, the algorithm in this paper has obvious advantages in signal detection accuracy and error detection rate on FH signal detection, and can be applied to the detection of UAV FH signal in the actual electromagnetic environment.

B. ANALYSIS OF PARAMETERS ESTIMATION

The following parameters are estimated by the results of those algorithms: dwell time, bandwidth, duration and span. As shown in Figure 29 and Figure 30, it is easy to find that when only UAV-A and UAV-B exist, the four parameters are obtained by the algorithm proposed in this paper are closer to the parameters of actual UAV. As shown in Figure 31 and Figure 32, when UAV-A and UAV-C exist at the same time,
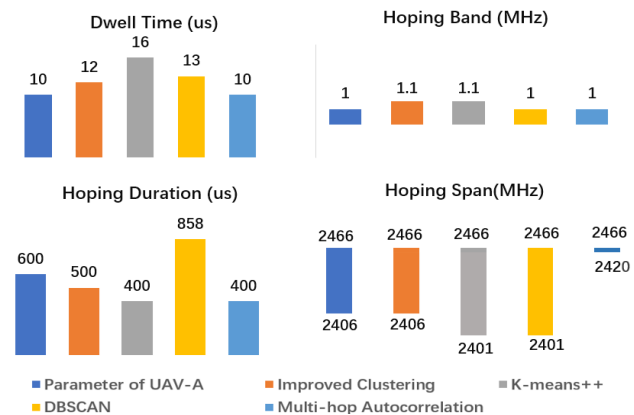

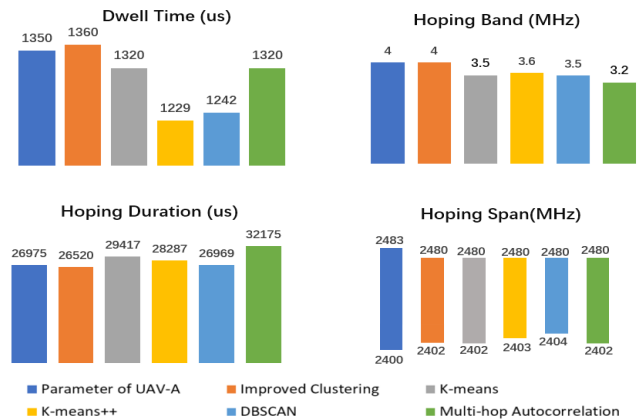**FIGURE 29.** Comparison and Analysis of UAV-A parameter estimation.

FIGURE 30. Comparison and Analysis of UAV-B parameter estimation.
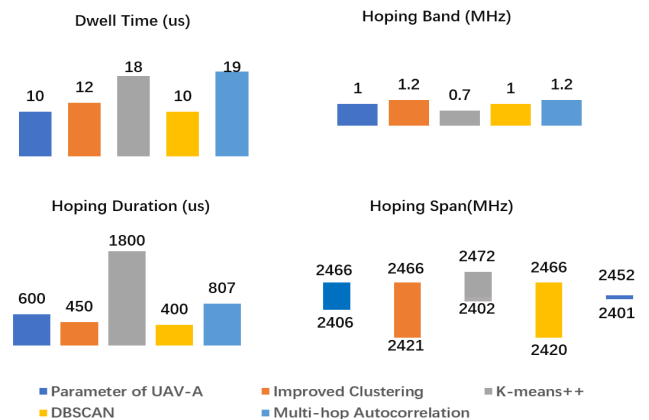
FIGURE 31. Parameter estimation of UAV-A under different algorithms.
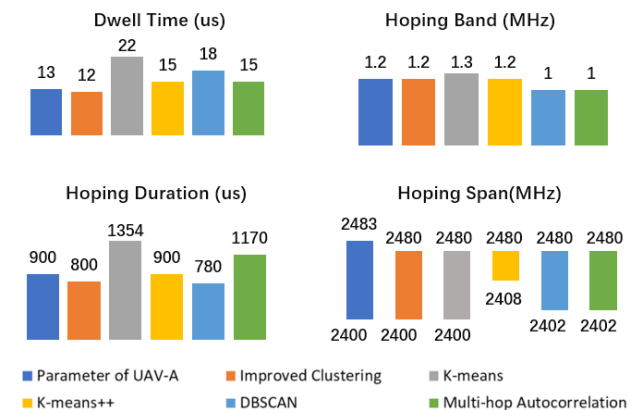
FIGURE 32. Parameter estimation of UAV-C under different algorithms.

the parameters obtained by the algorithm in this paper are also closer to the actual UAV parameters respectively. The detailed data are shown in Table 5, Table 6 and Table 7.

In the parameter estimation of UAV-A, due to the very short dwell time characteristics and maybe the limited amount of sampling data, it is impossible to detect and estimate the signal data of UAV-A using *K*-means.

When UAV-A and UAV-C exist at the same time, the parameter estimation of UAV-A after DBSCAN algorithm

TABLE 5. The performance analysis of UAV-A working parameter estimation.

Experiment conditions	Dwell Time (us)	Band (MHz)	Duration (us)	Span (MHz)
Parameter of UAV-A	10	1.0	600	2406-2466
Improved Clustering	12	1.1	500	2406-2466
K-means	—	—	—	—
K-means++	16	1.1	400	2401-2466
DBSCAN	13	1.0	858	2401-2466
Multi-hop Auto-correlation	10	1.0	400	2420-2466

TABLE 6. The performance analysis of UAV-B working parameter estimation.

Experiment conditions	Dwell Time (us)	Band (MHz)	Duration (us)	Span (MHz)
Parameter of UAV-A	1350	4	26975	2400-2483
Improved Clustering	1360	4	26520	2402-2480
K-means	1320	3.5	29417	2402-2480
K-means++	1229	3.6	28287	2403-2480
DBSCAN	1242	3.5	26969	2404-2480
Multi-hop Auto-correlation	1320	3.2	32175	2402-2480

TABLE 7. The performance analysis of UAV-A and UAV-C working parameter estimation.

	Experiment conditions	Dwell time (us)	Band (MHz)	Duration (us)	Span (MHz)
	Parameter of UAV-A	10	1.0	600	2406-2466
	Parameter of UAV-C	13	1.2	900	2400-2483
UAV-A	Improved Clustering	12	1.2	450	2421-2466
	K-means	—	—	—	—
	K-means++	18	0.7	1800	2402-2472
	DBSCAN	10	1.0	400	2420-2466
	Multi-hop Auto-correlation	19	1.2	807	2401-2452
UAV-C	Improved Clustering	12	1.2	800	2400-2480
	K-means	22	1.3	1354	2400-2480
	K-means++	15	1.2	900	2408-2480
	DBSCAN	18	1.0	780	2402-2480
	Multi-hop Auto-correlation	15	1.0	1170	2402-2480

is almost consistent with the actual parameters, which play a good performance. But when estimating the parameters of UAV-C, the proposed algorithm in this paper has a better estimation characteristic. In summary, the algorithm in this paper has a good and stable ability for FH signal analysis.

VI. CONCLUSION

In this paper, through adaptive noise threshold calculation, FH signal waveform characteristics and peak characteristics are developed. In different experimental environments, according to the pre-designed UAV signal detection process, the improved clustering analysis algorithm is used to detect, analyze and estimate the parameters of UAV FH signal in electromagnetic environment with low SNR. Compared with *K*-means, *K*-means^{++}, DBSCAN and Multi-hop Auto-correlation algorithm, the experimental results show that the proposed method can be used to quickly and effectively detect the FH signal of UAV, in addition, the estimated parameters are closer to the actual value. It seems that the proposed method is useful and alternative tool to study UAV signal detection and real-time tracking.

In experimental analysis, the proposed method and algorithm are suitable for detection and parameter estimation of the FH signal. Our future works will be focused on UAV signal source location and tracking.

REFERENCES

[1] Y. Zhang, "Research on 'illegal flying' of civil UAV," *Int. Core J. Eng.*, vol. 5, no. 7, pp. 254–259, 2019.

[2] H. Shakhatreh, A. H. Sawalmeh, A. Al-Fuqaha, Z. Dou, E. Almaita, I. Khalil, N. S. Othman, A. Khreishah, and M. Guizani, "Unmanned aerial vehicles (UAVs): A survey on civil applications and key research challenges," *IEEE Access*, vol. 7, pp. 48572–48634, 2019.

[3] A. Ranjan, H. B. Sahu, P. Misra, and B. Panigrahi, "Leveraging unmanned aerial vehicles in mining industry: Research opportunities and challenges," in *Unmanned Aerial Vehicles in Smart Cities*, F. Al-Turjman, Ed. Cham, Switzerland: Springer, 2020, doi: 10.1007/978-3-030-38712-9_7.

[4] S.-Y. Yun and S.-J. Park, "A study of foreign military UAV development trend and operational cases for the UAV developments of Republic of Korea Armed Forces," *J. Strategic Stud.*, vol. 25, no. 1, pp. 205–232, Mar. 2018.

[5] C. Li, P. Qi, D. Wang, and Z. Li, "On the anti-interference tolerance of cognitive frequency hopping communication systems," *IEEE Trans. Rel.*, vol. 69, no. 4, pp. 1453–1464, Dec. 2020.

[6] W.-J. Pan, C.-Y. Yang, T. Luan, Q.-H. Zuo, X.-L. Li, and J.-J. Zuo, "Optimization of China civil UAV regulations," in *Proc. Int. Conf. Comput., Electron. Commun. Eng. (CECE)*, 2017, pp. 1–5.

[7] W. Fu and T. Jiang, "A parameter estimation algorithm for multiple frequency-hopping signals based on compressed sensing," *Phys. Commun.*, vol. 37, Dec. 2019, Art. no. 100892.

[8] L. Wang, Z. Liu, Y. Feng, X. Liu, X. Xu, and X. Chen, "A parameter estimation method for time-frequency-overlapped frequency hopping signals based on sparse linear regression and quadratic envelope optimization," *Int. J. Commun. Syst.*, vol. 33, no. 12, p. e4463, Aug. 2020.

[9] N.-K. Kim and S.-J. Oh, "Comparison of methods for parameter estimation of frequency hopping signals," in *Proc. Int. Conf. Inf. Commun. Technol. Converg. (ICTC)*, Jeju, South Korea, Oct. 2017, pp. 567–569.

[10] J. Ma, Y. Yang, H. Li, and J. Li, "FH-BOC: Generalized low-ambiguity anti-interference spread spectrum modulation based on frequency-hopping binary offset carrier," *GPS Solutions*, vol. 24, no. 3, pp. 227–246, Jul. 2020.

[11] P. Huang, "New class of optimal frequency-hopping sequence based on cyclotomy," in *Proc. 13th Int. Comput. Conf. Wavelet Act. Media Technol. Inf. Process. (ICCWAMTIP)*, Chengdu, China, Dec. 2016, pp. 86–89.

[12] M. T.-D. Cruz, W. K. Mahdloom, and S. Suresh, "Networks coexistence with other 2.4 GHz ISM devices," *Int. J. Trend Sci. Res. Develop.*, vol. 1, no. 7, 2018.

[13] G. Fu, D. X. Zhu, and Y. Feng, "Research on frequency hopping parameters of hybrid spread spectrum signal," *Appl. Mech. Mater.*, vols. 543–547, pp. 2551–2554, Mar. 2014.

[14] Z. Lei, P. Yang, and L. Zheng, "Detection and frequency estimation of frequency hopping spread spectrum signals based on channelized modulated wideband converters," *Electronics*, vol. 7, no. 9, p. 170, Aug. 2018.

[15] Y. Wang, C. Zhang, and F. Jing, "Frequency-hopping signal parameters estimation based on orthogonal matching pursuit and sparse linear regression," *IEEE Access*, vol. 6, pp. 54310–54319, 2018.

[16] D. Angelosante, G. B. Giannakis, and N. D. Sidiropoulos, "Estimating multiple frequency-hopping signal parameters via sparse linear regression," *IEEE Trans. Signal Process.*, vol. 58, no. 10, pp. 5044–5056, Oct. 2010.

[17] Y. He, Y. Su, Y. Chen, Y. Yu, and X. Yang, "Double window spectrogram difference method: A blind estimation of frequency-hopping signal for battlefield communication environment," in *Proc. 24th Asia–Pacific Conf. Commun. (APCC)*, Ningbo, China, Nov. 2018, pp. 439–443.

[18] J. Xie, S. Hou, and Q. Zhang, "An improved central frequency estimation method for frequency-hopping signal," in *Proc. IEEE Int. Conf. Power, Intell. Comput. Syst. (ICPICS)*, Shenyang, China, Jul. 2019, pp. 250–253.

[19] Y. Wang, Y. Lin, and X. Chi, "A parameter estimation method of frequency hopping signal based on sparse time-frequency method," in *Proc. IEEE 23rd Int. Conf. Digit. Signal Process. (DSP)*, Shanghai, China, Nov. 2018, pp. 1–5.

[20] K.-G. Lee and S.-J. Oh, "Detection of fast frequency-hopping signals using dirty template in the frequency domain," *IEEE Wireless Commun. Lett.*, vol. 8, no. 1, pp. 281–284, Feb. 2019.

[21] K.-G. Lee and S.-J. Oh, "Detection of frequency-hopping signals with deep learning," *IEEE Commun. Lett.*, vol. 24, no. 5, pp. 1042–1046, May 2020.

[22] W. Rui and W. Wei, "Research on anti-jamming method of frequency hopping communication based on blind source separation in complex electromagnetic environment," in *Proc. Int. Conf. Smart Grid Electr. Automat. (ICSGEA)*, Xiangtan, China, Aug. 2019, pp. 378–381.

[23] N. Saulig, J. Lerga, Z. Baracskai, and M. Dakovic, "Adaptive thresholding in extracting useful information from noisy time-frequency distributions," in *Proc. 11th Int. Symp. Image Signal Process. Anal. (ISPA)*, Dubrovnik, Croatia, Sep. 2019, pp. 329–334.

[24] X. Shen, Y. Ma, J. Yu, W. Wang, J. Huo, J. Cui, and S. Cheng, "Dynamic threshold based target signal cooperative extraction method for high frequency electromagnetic environment measurement," in *Proc. 3rd IEEE Int. Conf. Control Sci. Syst. Eng. (ICCSSE)*, Beijing, China, Aug. 2017, pp. 552–555.

[25] B. Kaplan, İ. Kahraman, A. Görçin, H. A. Çirpan, and A. R. Ektin, "Measurement based FHSS–type drone controller detection at 2.4 GHz: An STFT approach," in *Proc. IEEE 91st Veh. Technol. Conf. (VTC-Spring)*, Antwerp, Belgium, May 2020, pp. 1–6.

[26] J. Wan, D. Zhang, W. Xu, and Q. Guo, "Parameter estimation of multi frequency hopping signals based on space-time-frequency distribution," *Symmetry*, vol. 11, no. 5, p. 648, May 2019.

[27] A. Kanaa and A. Z. Sha'ameri, "A robust parameter estimation of FHSS signals using time–frequency analysis in a non-cooperative environment," *Phys. Commun.*, vol. 26, pp. 9–20, Feb. 2018.

[28] L. Zuo, J. Pan, and B. Ma, "Parameter estimation of multiple frequency-hopping signals with two sensors," *Sensors*, vol. 18, no. 4, p. 1088, Apr. 2018.

[29] J. Su, R. Xu, S. Yu, B. Wang, and J. Wang, "Idle slots skipped mechanism based tag identification algorithm with enhanced collision detection," *KSII Trans. Internet Inf. Syst.*, vol. 14, no. 5, pp. 2294–2309, 2020.

[30] J. Su, R. Xu, S. Yu, B. Wang, and J. Wang, "Redundant rule detection for software-defined networking," *KSII Trans. Internet Inf. Syst.*, vol. 14, no. 6, pp. 2735–2751, 2020.

[31] B. Zhang, D. Ji, D. Fang, S. Liang, Y. Fan, and X. Chen, "A novel 220-GHz GaN on-chip tripler with high driven power," *IEEE Electron Device Lett.*, vol. 40, no. 5, pp. 780–783, May 2019.

[32] Z. Niu, D. Li, B. Zhang, K. Yang, Y. Yang, D. Ji, Y. Liu, Y. Feng, Y. Fan, and X. Chen, "Mode analyzing method for fast design of branch waveguide coupler," *IEEE Trans. Microw. Theory Techn.*, vol. 67, no. 12, pp. 4733–4740, Dec. 2019.

JING GAO received the master's degree in electronic and communication engineering from the Chengdu University of Technology, in June 2013. He is currently an Assistant Researcher with the Second Research Institute of Civil Aviation Administration of China. His main research interest includes civil aviation radio technology.

GUOMIN ZHANG received the master's degree in software engineering from Xihua University, Chengdu, Sichuan, China, in June 2019. He is currently working for a company as a Software Development Engineer, responsible for system architecture design and implementation. His main research interests include spectrum signal processing and data analysis.

MINGMING KONG received the M.S. degree in applied mathematics from Xihua University, Chengdu, China, in December 2010. He is currently an Associate Professor with the School of Computer and Software Engineering, Xihua University. His current research interests include intelligent information processing and spectrum management.

JIAQUAN YE received the M.B.A. degree from Sichuan Normal University, in June 2013. He is currently a Researcher with the Second Research Institute of Civil Aviation Administration of China, and also an Expert in the field of civil aviation technology and ATC. He has published 18 academic journals or conferences. His research interests include civil aviation communication, navigation, surveillance, and related air traffic control technology fields.

ZHENG PEI received the M.S. and Ph.D. degrees from Southwest Jiaotong University, Chengdu, China, in 1999 and 2002, respectively. He is currently a Professor with the School of Computer and Software Engineering, Xihua University, Chengdu. He has published nearly 70 research papers in academic journals or conferences. His research interests include rough set theory, fuzzy set theory, logical reasoning, and linguistic information processing.

JIE ZOU received the bachelor's degree in communication engineering from Southwest Jiaotong University, Chengdu, China, in June 2007. He is currently an Associate Researcher with the Second Research Institute of Civil Aviation Administration of China. His main research interests include civil aviation air traffic control technology and civil aviation radio technology.

KAITAO CUI received the master's degree in control theory and engineering from Xihua University, in May 2015. He is currently a Research Assistant Professor with the Second Research Institute of Civil Aviation Administration of China. His main research interests include aeronautical radio technology and spectrum management.

• • •